

Supporting Information

Coupling Efficient Biomass Upgrading with H₂ Production via Bifunctional Cu_xS@NiCo-LDHs Core-Shell Nanoarray Electrocatalysts

Xiaohui Deng,^a Xiaomin Kang,^a Mei Li,^a Kun Xiang,^a Cheng Wang,^a ZaiPing Guo,^b Jiujun Zhang,^c Xian-Zhu Fu,^{*a} Jing-Li Luo ^{*a,d}

^a College of Materials Science and Engineering, Shenzhen University, Shenzhen, 518060, China. E-mail: xz.fu@szu.edu.cn.

^b Institute for Superconducting and Electronic Materials School of Mechanical, Materials, Mechatronic and Bio-medical Engineering University of Wollongong NSW 2500, Australia

^c Institute for Sustainable Energy/College of Sciences, Shanghai University, Shanghai, 200444, China

^d Department of Chemical and Materials Engineering, University of Alberta, Edmonton, Alberta T6G 1H9, Canada. E-mail: Jingli.luo@ualberta.ca

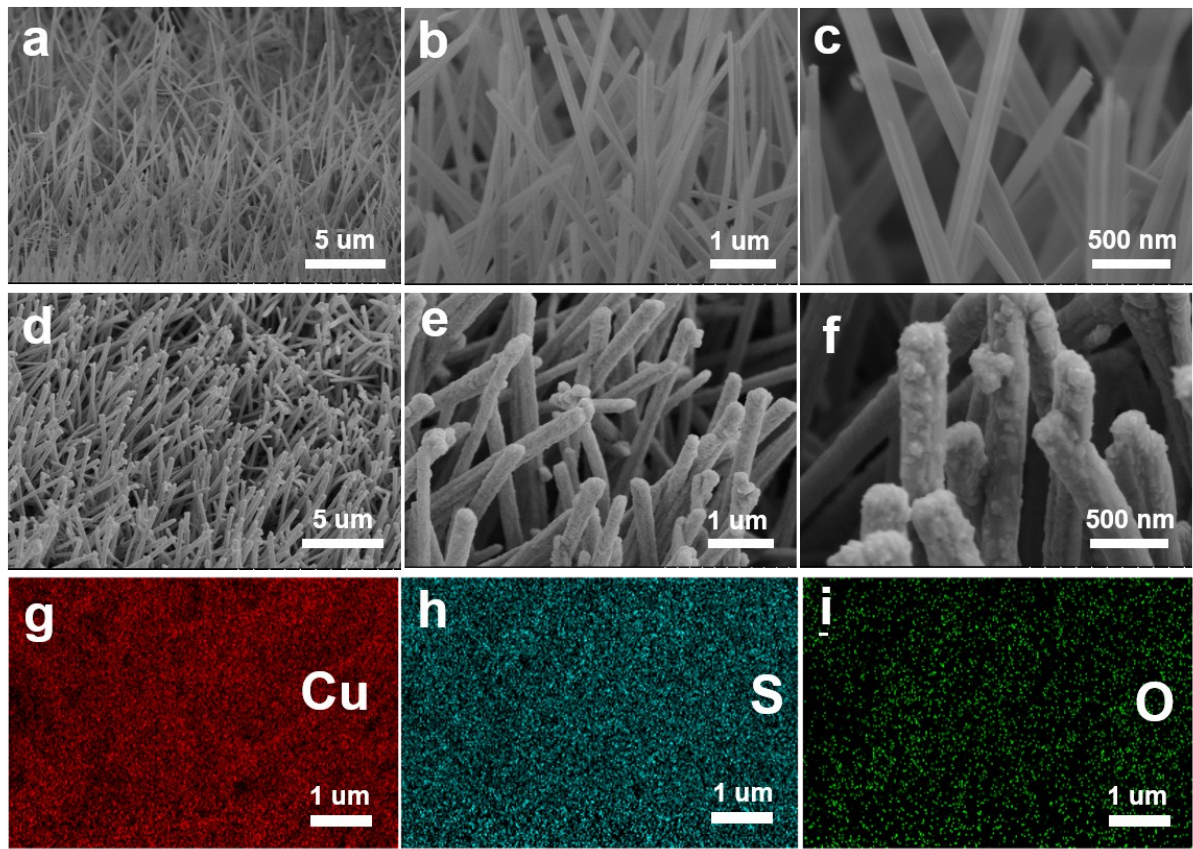


Figure S1. SEM images of Cu(OH)₂ NAs/CF (a, b, c), Cu_xS NAs/CF (d, e, f) and elemental mappings of Cu, S and O (g, h, i).

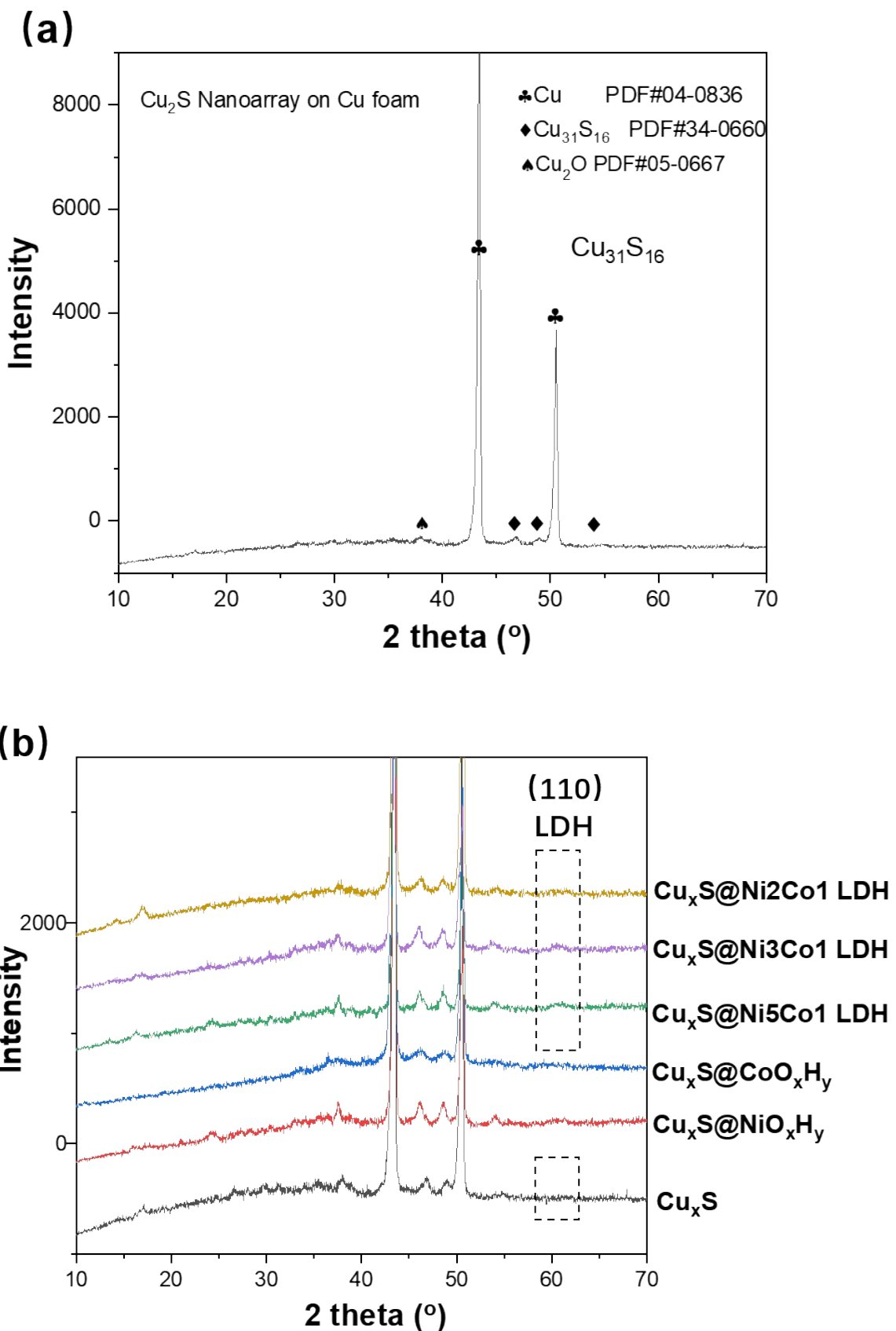


Figure S2. XRD patterns of (a) Cu_xS NAs/CF and (b) as-prepared Cu_xS@NiO_xH_y, Cu_xS@CoO_xH_y and Cu_xS@NiCo LDHs.

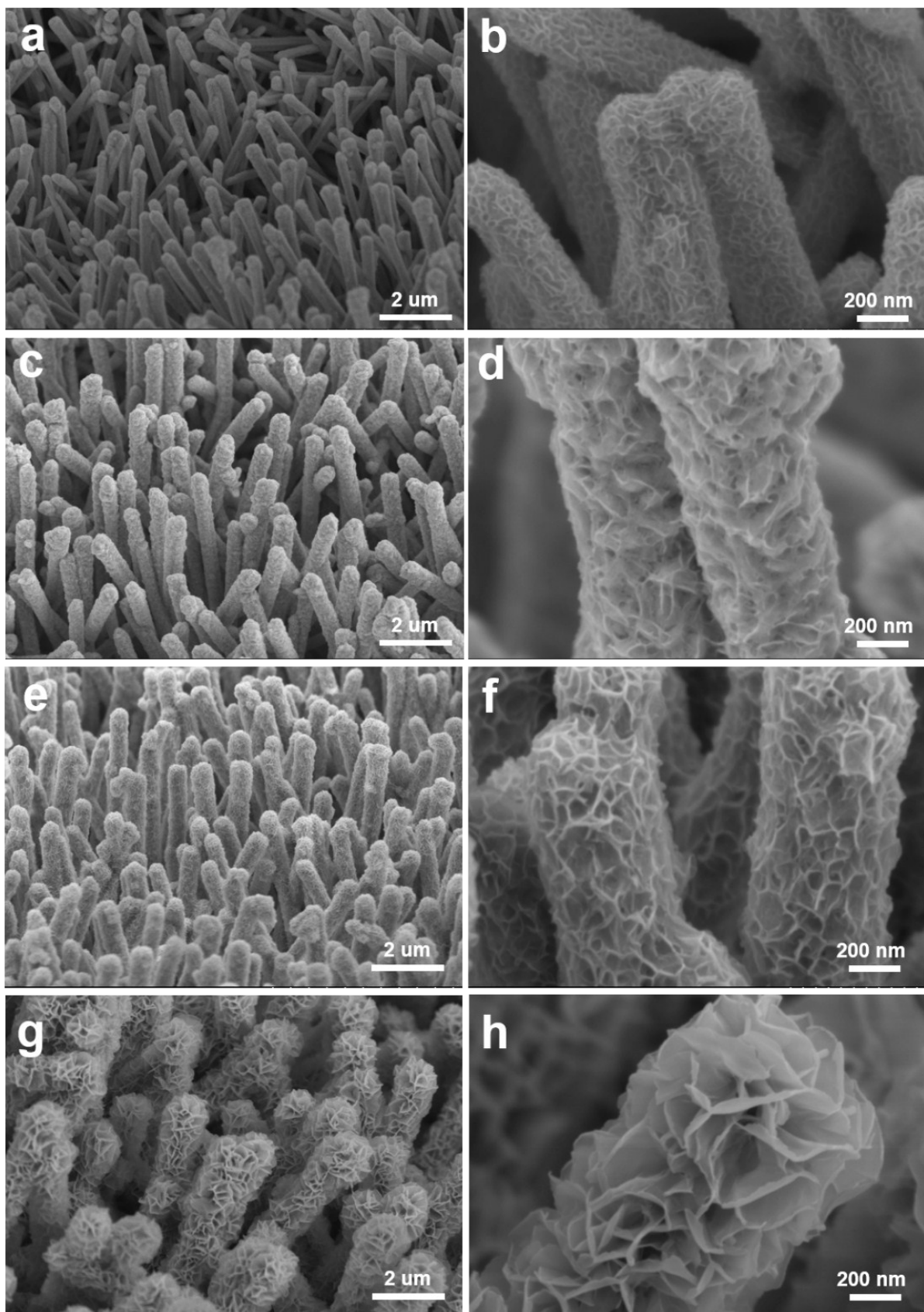


Figure S3. SEM images of (a, b) $\text{Cu}_x\text{S}@{\text{NiO}_m\text{H}_n}$, (c, d) $\text{Cu}_x\text{S}@{\text{Ni}_{0.83}\text{Co}_{0.17}\text{O}_m\text{H}_n}$, (e, f) $\text{Cu}_x\text{S}@{\text{Ni}_{0.67}\text{Co}_{0.33}\text{O}_m\text{H}_n}$ and (g, h) $\text{Cu}_x\text{S}@{\text{CoO}_m\text{H}_n}$.

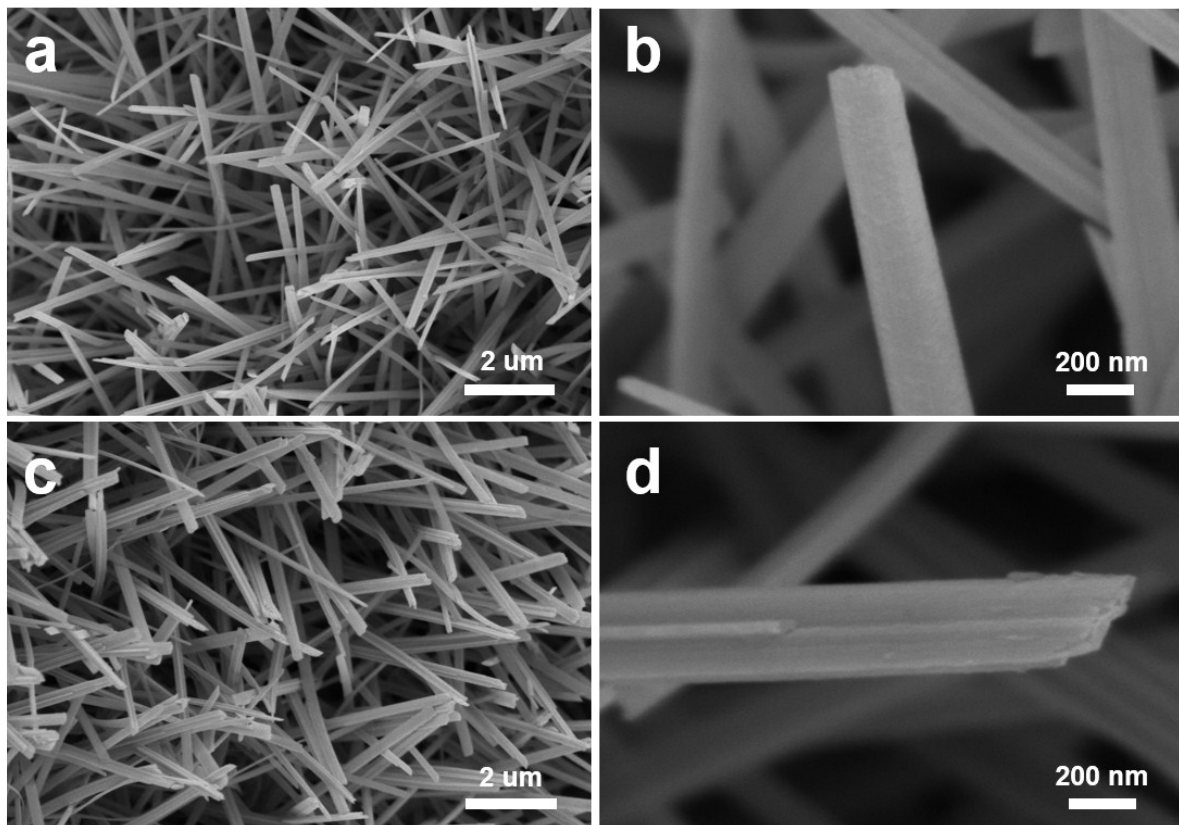


Figure S4. SEM images showing unsuccessful electrodeposition of $\text{Ni}_{0.75}\text{Co}_{0.25}\text{-LDH}$ and $\text{Co}(\text{OH})_2$ when $\text{Cu}(\text{OH})_2$ NAs/CF were used as substrate. Without the sulfidation step the electrodeposition resulted in inhomogeneous electrode and large portion of the nanowires were not coated.

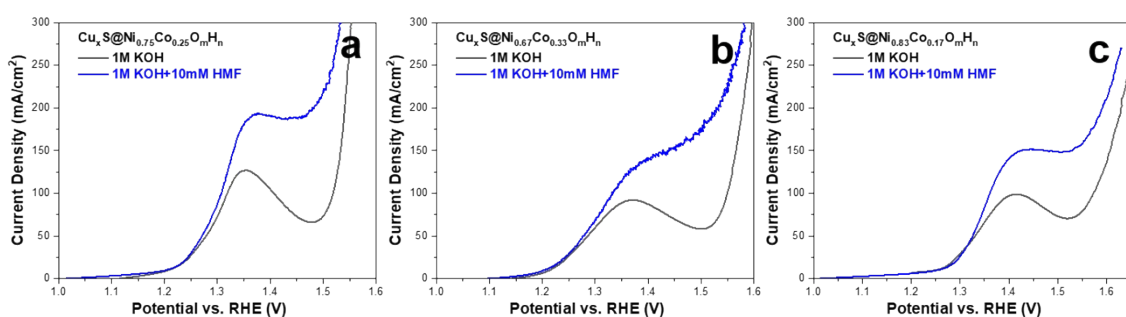


Figure S5. LSV curve comparisons of electrochemical HMF Oxidation (blue) and H_2O oxidation (black) catalyzed by $\text{Cu}_x\text{S}@\text{Ni}_{0.75}\text{Co}_{0.25}\text{O}_m\text{H}_n$, $\text{Cu}_x\text{S}@\text{Ni}_{0.67}\text{Co}_{0.33}\text{O}_m\text{H}_n$ and $\text{Cu}_x\text{S}@\text{Ni}_{0.83}\text{Co}_{0.17}\text{O}_m\text{H}_n$.

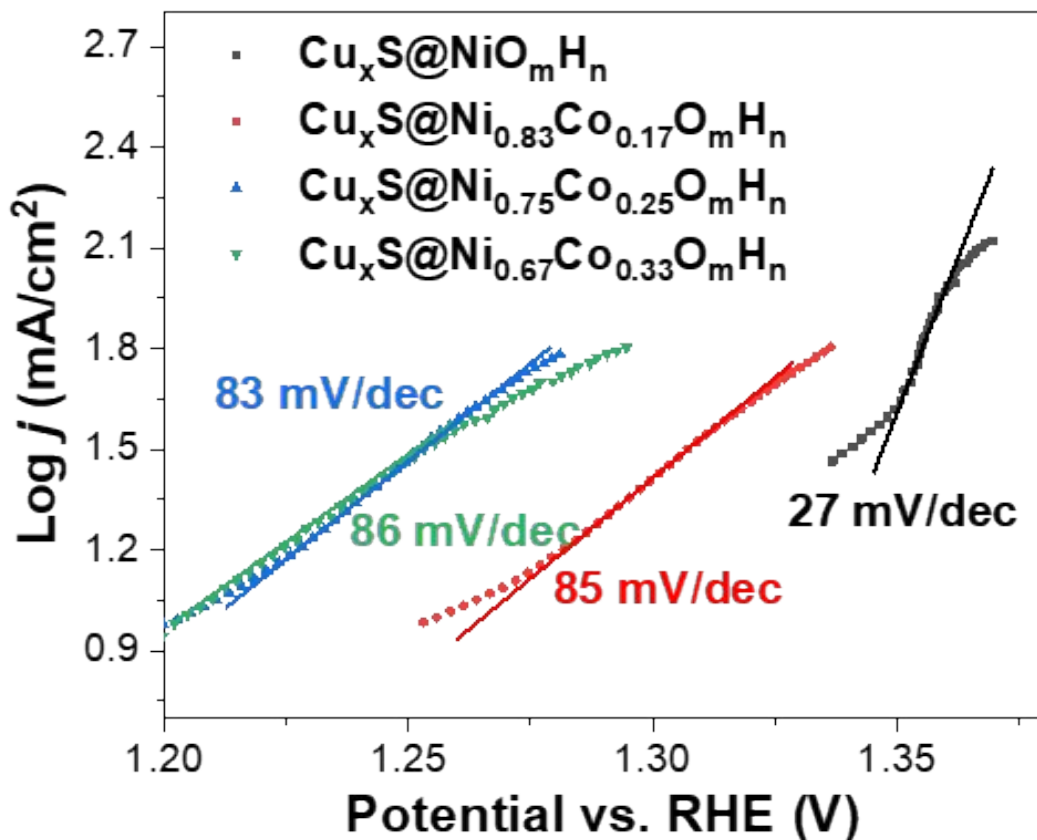


Figure S6. Tafel plots of as-prepared core-shell composites with various Ni to Co ratio towards HMF oxidation.

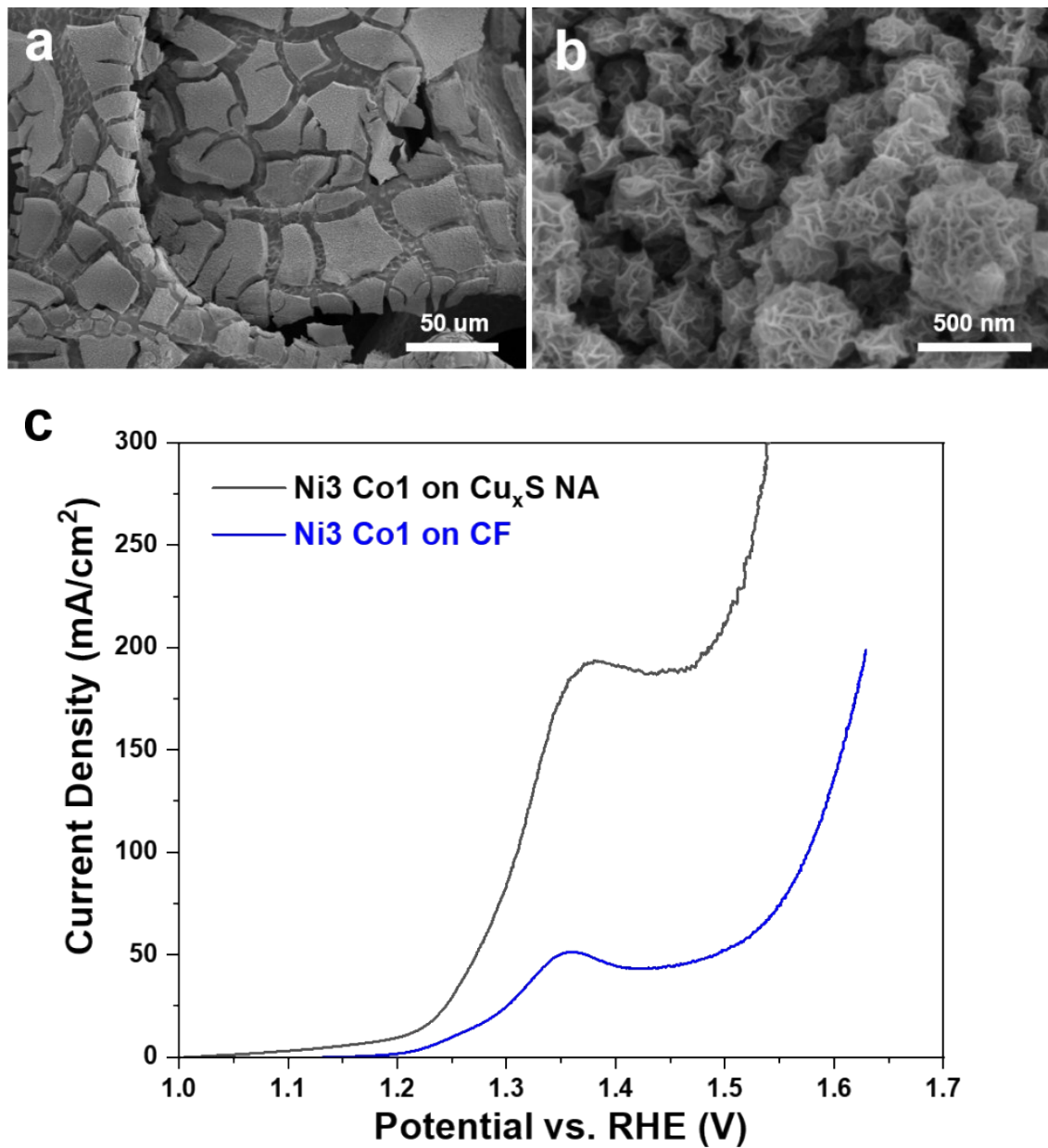


Figure S7. a, b) SEM images of electrodeposited $\text{Ni}_{0.75}\text{Co}_{0.25}\text{O}_m\text{H}_n$ on copper foam. c) Comparison of electrochemical HMF oxidation activity of $\text{Ni}_{0.75}\text{Co}_{0.25}\text{O}_m\text{H}_n/\text{CF}$ and $\text{Cu}_x\text{S}@\text{Ni}_{0.75}\text{Co}_{0.25}\text{O}_m\text{H}_n$.

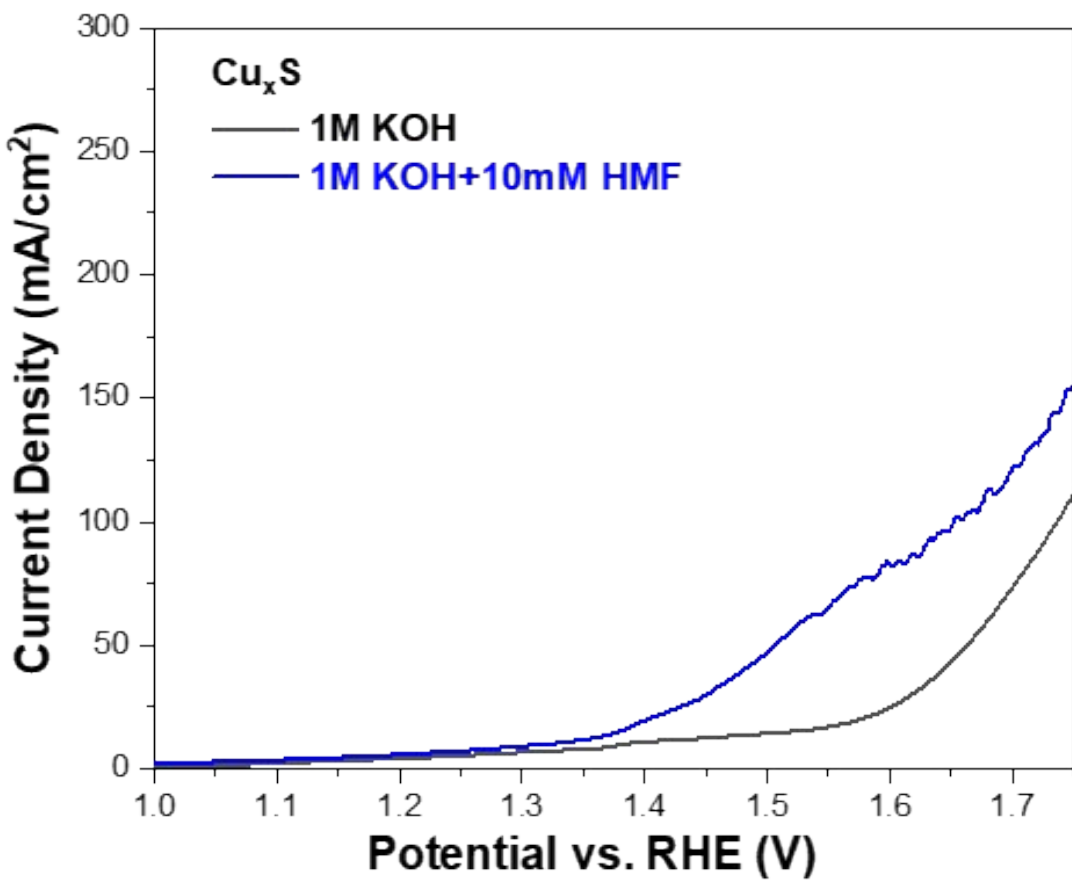


Figure S8. LSV curve comparisons of electrochemical HMF Oxidation (blue) and H₂O oxidation (black) catalyzed by Cu_xS NAs/CF.

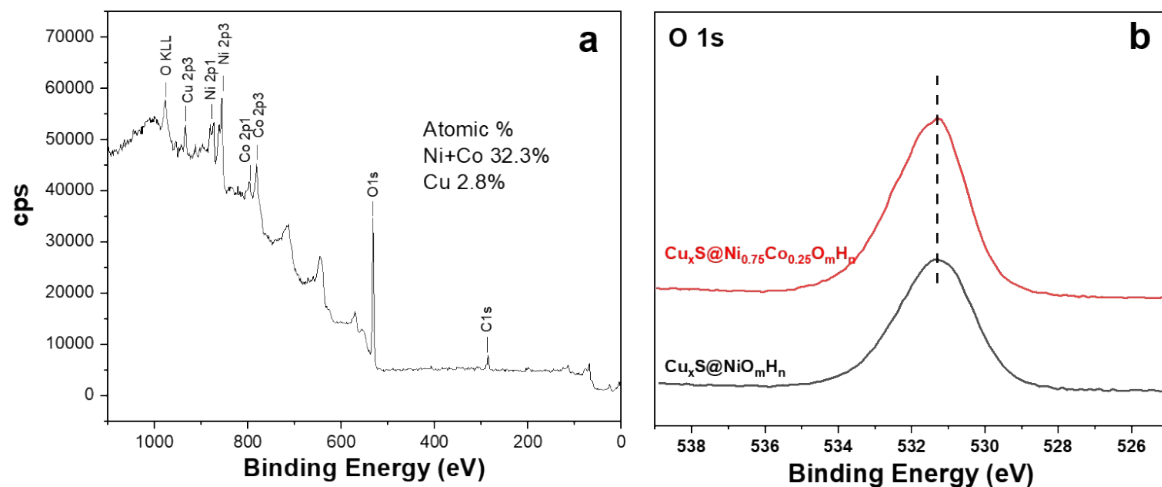


Figure S9. a) Full-range XPS spectra of $\text{Cu}_x\text{S}@\text{Ni}_{0.75}\text{Co}_{0.25}\text{O}_m\text{H}_n$. b) O1s spectra of $\text{Cu}_x\text{S}@\text{NiO}_m\text{H}_n$ and $\text{Cu}_x\text{S}@\text{Ni}_{0.75}\text{Co}_{0.25}\text{O}_m\text{H}_n$.

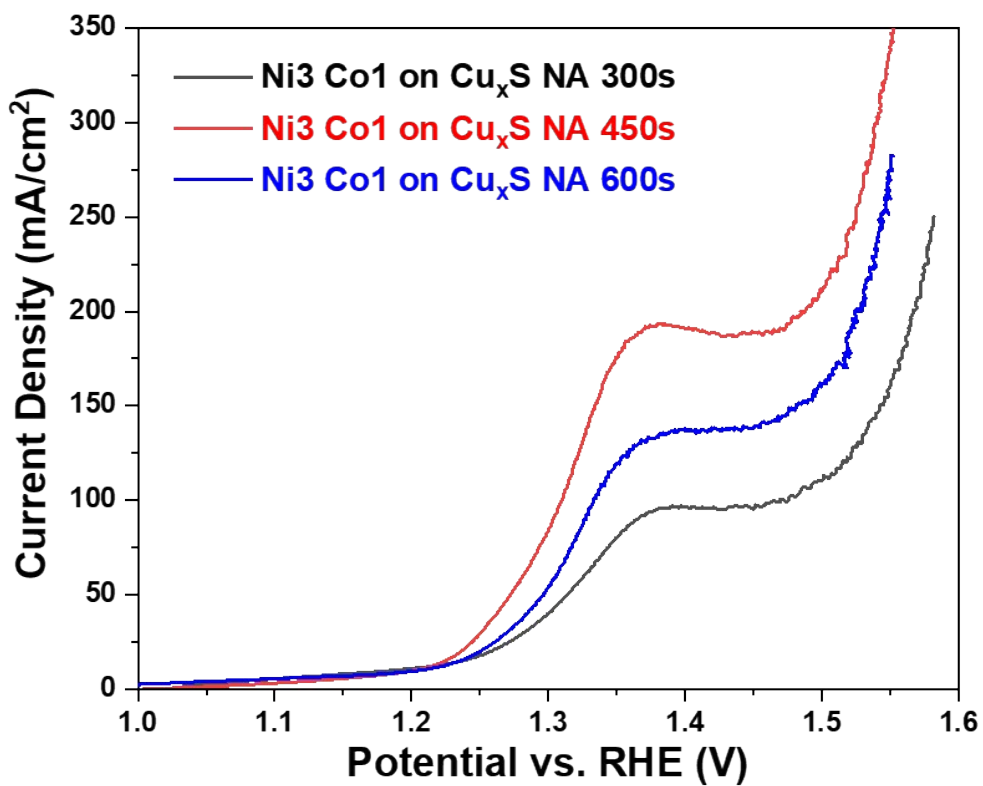


Figure S10. LSV curves of electrochemical HMF oxidation catalyzed by $\text{Cu}_x\text{S}@\text{Ni}_{0.75}\text{Co}_{0.25}\text{O}_m\text{H}_n$ with various electrodeposition time.

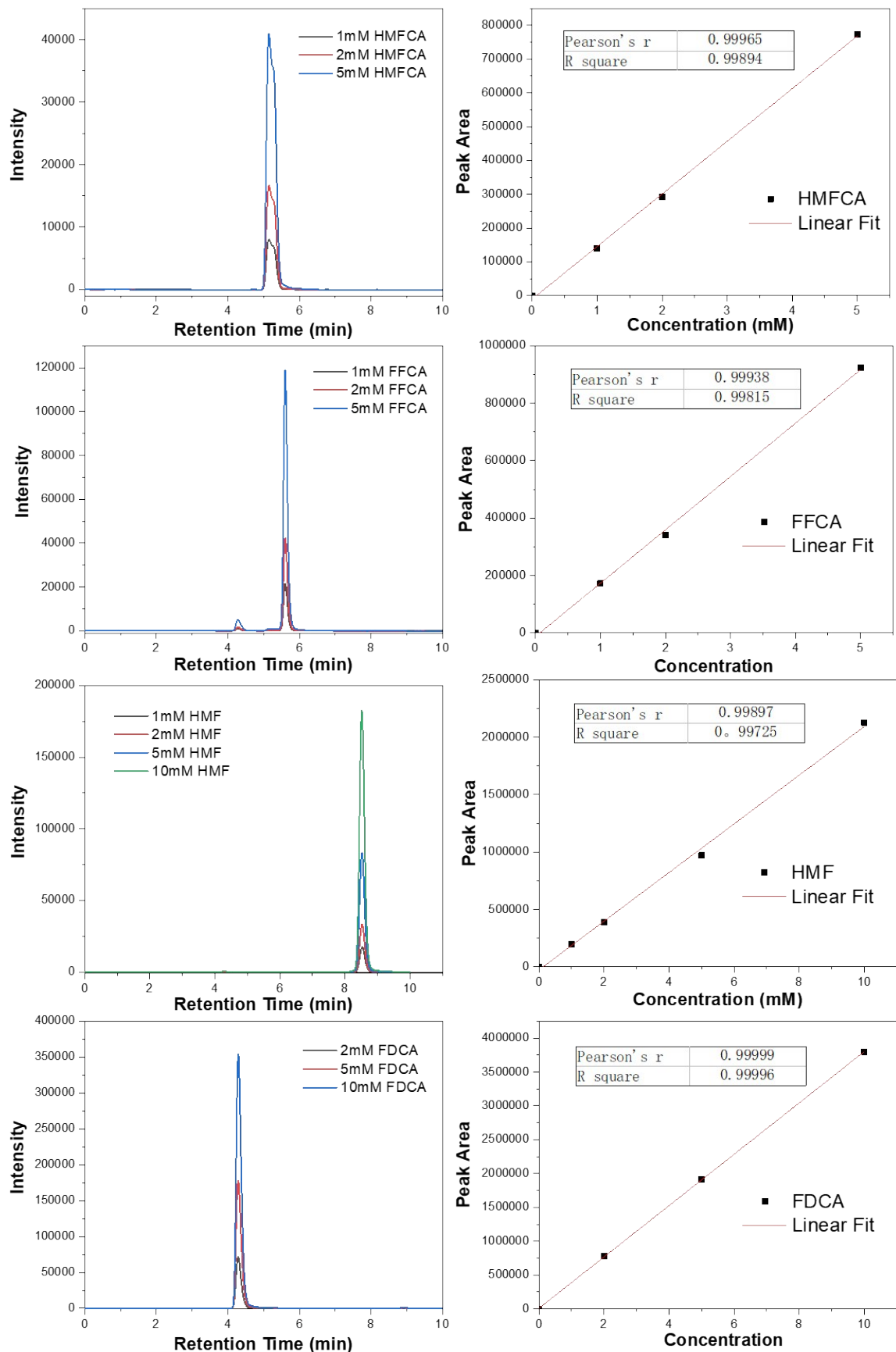


Figure S11. Reference HPLC spectra and calibration curves for HMFCA, FFCA, HMF and FDCA.

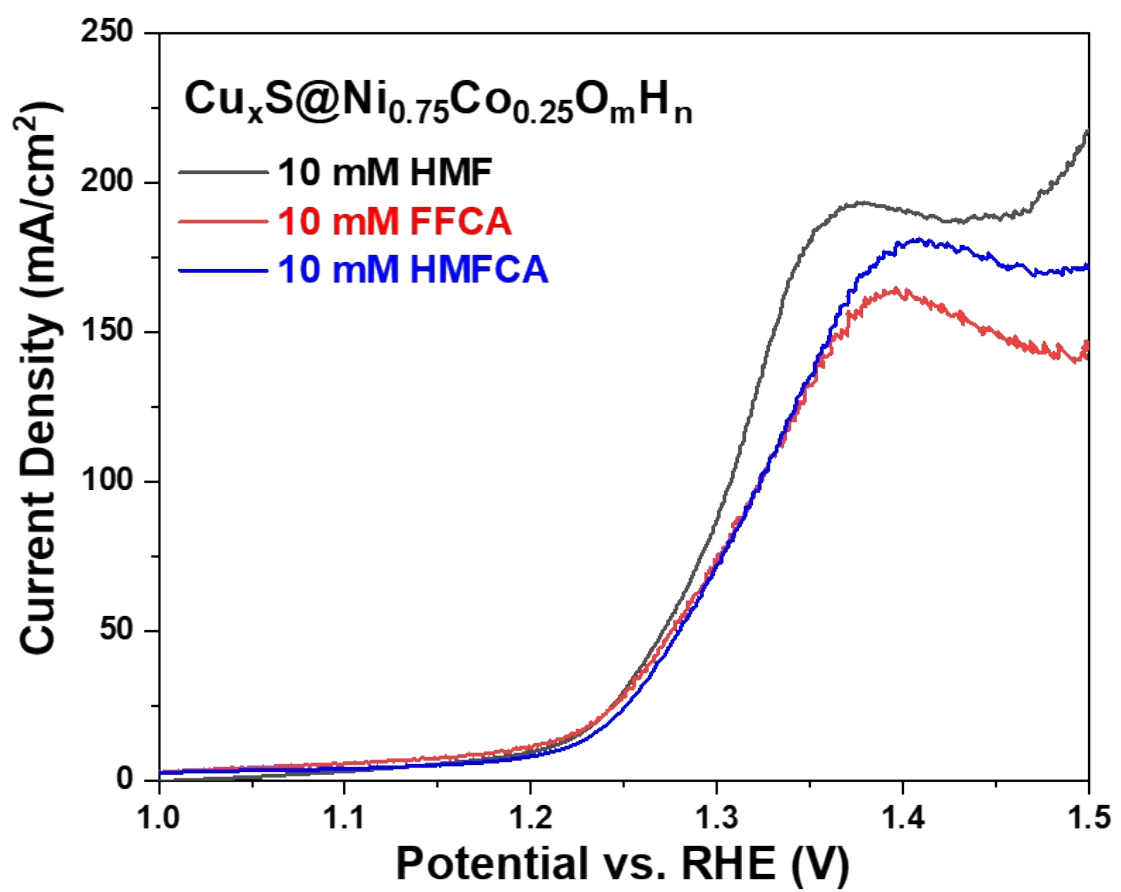


Figure S12. LSV curve comparison of HMF, FFCA and HMFCA oxidation catalyzed by Cu_xS@Ni_{0.75}Co_{0.25}O_mH_n.

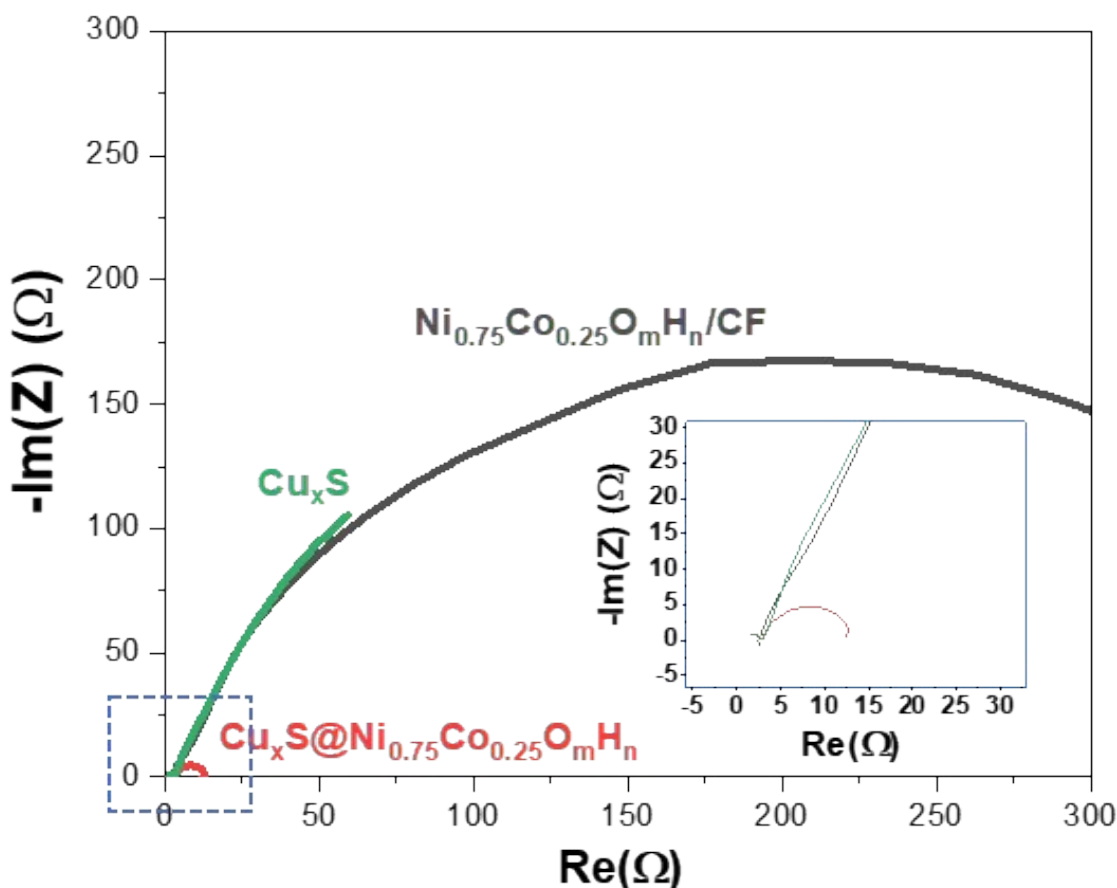
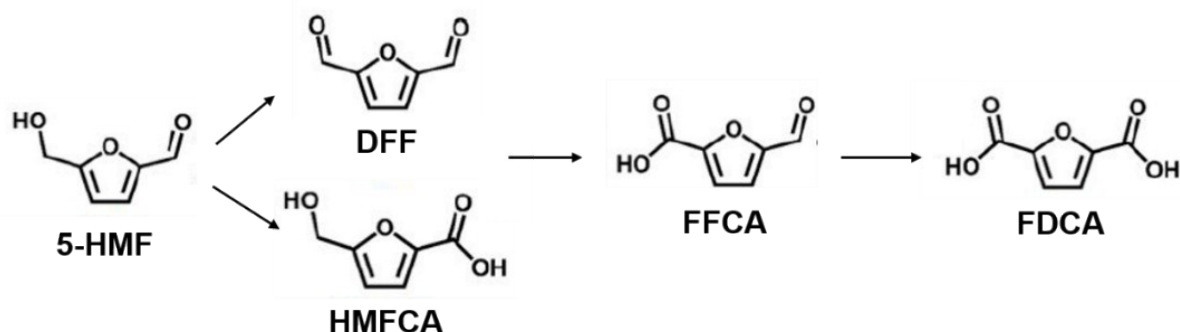


Figure S13. Nyquist plots of Cu_xS , $\text{Cu}_x\text{S}@(\text{Ni}_{0.75}\text{Co}_{0.25}\text{O}_m\text{H}_n)$ and $\text{Ni}_{0.75}\text{Co}_{0.25}\text{O}_m\text{H}_n$ electrodeposited on copper foam (@-1.1 V vs Hg/HgO). The inset is the enlarged EIS plots of the square region.



Scheme S1. Proposed reaction pathways of 5-HMF oxidation.

Table S1. Atomic percentage of O, S and Cu as obtained from the EDX measurements.

Element	wt%	wt% Sigma	Atom%
O	2.04	0.12	6.52
S	18.60	12.04	29.65
Cu	79.36	0.17	63.83
Total	100.00		100.00

Table S2. Ni/Co ratio in prepared Cu_xS@NiCo LDHs as determined by ICP-OES.

Samples	Theoretical Ni/Co	Measured Ni/Co by ICP-OES
Cu _x S@Ni _{0.83} Co _{0.17} O _m H _n	83.3%/16.7%	85.7%/14.3%
Cu _x S@Ni _{0.75} Co _{0.25} O _m H _n	75%/25%	74.3%/25.7%
Cu _x S@Ni _{0.67} Co _{0.33} O _m H _n	66.7%/33.3%	68.4%/31.6%

Table S3. Comparison of electrocatalytic activity towards HMF/organic substrate oxidation for recently reported electrocatalysts.

Electrode materials	Electrolyte/ Oxidized substrate	^a Current density at 1.3 V vs RHE (mA/cm ²)	^b Current density at 1.4 V vs RHE (mA/cm ²)	Tafel Slope (mV/dec)	Reference
Ni _x B/Nickel Foam (NF)	1 M KOH/ 10 mM HMF	0 (onset at ~ 1.38 V)	~ 10	-	1
CoxB/NF	1 M KOH/ 10 mM HMF	~ 3	~ 22	-	2
Ni ₂ P/NF	1 M KOH/ 10 mM HMF	0 (onset at ~ 1.36 V)	> 200	-	3
Ni ₃ S ₂ /NF	1 M KOH/ 10 mM HMF	0	~ 200	-	4
NiFe LDH/Carbon Fiber Paper	1 M KOH/ 10 mM HMF	~ 10	~ 90	75	5
NiCo ₂ O ₄ nanoarrays/NF	1 M KOH/ 10 mM HMF	~ 1.5	~ 3.5	135.7	6
Co-P/CF	1 M KOH/ 50 mM HMF	~ 2	~ 50	-	7
NiSe/NF	1 M KOH/ 10 mM amines	0	~ 170	-	8
Cu _x S@NiO _m H _n	1 M KOH/ 10 mM HMF	15.6	189.7	24	This work
Cu _x S@CoO _m H _n	1 M KOH/ 10 mM HMF	11.4	80.0	188	This work
Cu _x S@Ni _{0.75} Co _{0.25} O _m H _n	1 M KOH/ 10 mM HMF	87.6	^c 187 @ 1.36 V	83	This work

^{a,b} It should be mentioned that these values are not provided in most cases, therefore they are read from the figures in the corresponding publication.

^c As can be observed from the linear scan, the oxidation current is likely limited by the mass transport and does not increase after this potential.

Table S4. Comparison of electrocatalytic activity towards hydrogen evolution reaction for recently reported transition metal-based electrocatalysts.

Electrode materials	Electrolyte	Overpotential @ 10 mA/cm ² (mV)	Tafel Slope (mV/dec)	Reference
Au doped-Ni Co hydroxide	1 M KOH	200	92	9
Cu@NiFe LDH/CF	1 M KOH	116	58.9	10
NiCoP _x	1 M KOH	63	34.3	11
NiFe LDH/CeO _x /NF	1 M KOH	154	101	12
CoP/CC	1 M KOH	209	129	13
Ni _{4.3} Co _{4.7} S ₈	1 M KOH	148	90	14
CoS _x ultrathin nanosheets	1 M KOH	127	117	15
Co _{5.47} N NP@N-doped porous carbon	1 M KOH	149	86	16
TiO ₂ @Co ₉ S ₈	1 M KOH	139	65	17
NiFeO _x @NiCu alloy	1 M KOH	66	67.8	18
(NiCo) _{0.85} Se	1 M KOH	169	115.6	19
Cu_xS@Ni_{0.75}Co_{0.25}O_mH_n	1 M KOH	107	35	This work

Table S5. Performance comparison of reported two-electrode electrolyzer coupling novel anodic reactions and hydrogen production.

Electrode materials	Anodic Reaction	Cell Voltage @ 10 mA/cm ² (V)	Cell Voltage @ 50 mA/cm ² (V)	Cell Voltage @ 100 mA/cm ² (V)	Reference
Ni ₂ P/Nickel Foam (NF) Ni ₂ P/Nickel Foam (NF)	HMF Oxidation	1.44	1.58	-	3
Ni ₃ S ₂ /NF Ni ₃ S ₂ /NF	HMF Oxidation	1.46	1.58	1.64	4
NiSe/NF CoP	Primary Amines Oxidation	~1.44	-	-	8
NiMoO-Ar/NF NiMoO-H ₂ /NF	Urea Oxidation	1.38	1.48	1.55	20
Cu _x S@Ni _{0.75} Co _{0.25} O _m H _n Cu _x S@Ni _{0.75} Co _{0.25} O _m H _n	HMF Oxidation	1.34	1.49	1.58	This work

References

- [1] Barwe, S.; Weidner, J.; Cychy, S.; Morales, D. M.; Dieckhöfer, S.; Hiltrop, D.; Masa, J.; Muhler, M.; Schuhmann, W. *Angew. Chem. Int. Ed.* 2018, **57**, 11460-11464.
- [2] Weidner, J.; Barwe, S.; Slizberg, K.; Piontek, S.; Masa, J.; Apfel, U. P.; Schuhmann, W. *Beilstein J. Org. Chem.* 2018, **14**, 1436-1445.
- [3] You, B.; Jiang, N.; Liu, X.; Sun, Y. *Angew. Chem. Int. Ed.* 2016, **55**, 9913-9917.
- [4] You, B.; Liu, X.; Jiang, N.; Sun, Y. *J. Am. Chem. Soc.* 2016, **138**, 13639-13646.
- [5] Liu, W. J.; Dang, L. N.; Xu, Z. R.; Yu, H. Q.; Jin, S.; Huber, G. W. *ACS Catal.* 2018, **8**, 5533-5541.
- [6] Kang, M. J.; Park, H.; Jegal, J.; Hwang, S. Y.; Kang, Y. S.; Cha, H. G. *Appl. Catal. B-Environ.* 2019, **242**, 85-91.
- [7] Jiang, N.; You, B.; Boonstra, R.; Terrero Rodriguez, I. M.; Sun, Y. *ACS Energy Lett.* 2016, **1**, 386-390.
- [8] Huang, Y.; Chong, X. D.; Liu, C. B.; Liang, Y.; Zhang, B. *Angew. Chem. Int. Ed.* 2018, **57**, 13163-13166.
- [9] Sultana, U. K.; Riches, J. D.; O'Mullane A. P., *Adv. Funct. Mater.* 2018, **28**, 1804361.
- [10] Yu, L.; Zhou, H. Q.; Sun, J. Y.; Qin, F.; Yu, F.; Bao, J. M.; Yu, Y.; Chen, S.; Ren, Z. F. *Energy Environ. Sci.* 2017, **10**, 1820-1827.
- [11] Zhang, R.; Wang, X. X.; Yu, S. J.; Wen, T.; Zhu, X. W.; Yang, F. X.; Sun, X. N.; Wang, X. K.; Hu, W. P. *Adv. Mater.* 2017, **29**, 1605502.
- [12] Wang, X.; Yang, Y.; Diao, L.; Tang, Y.; He, F.; Liu, E.; He, C.; Shi, C.; Li, J.; Sha, J.; Ji, S.; Zhang, P.; Ma, L.; Zhao, N. *ACS Appl. Mater. Interfaces* 2018, **10**, 35145-35153.
- [13] Tian, J. Q.; Liu, Q.; Asiri, A. M.; Sun, X. P. *J. Am. Chem. Soc.* 2014, **136**, 7587-7590.
- [14] Tang, Y.; Yang, H.; Sun, J.; Xia, M.; Guo, W.; Yu, L.; Yan, J.; Zheng, J.; Chang, L.; Gao, F. *Nanoscale* 2018, **10**, 10459-10466.
- [15] Zhu, K.; Wu, T.; Li, M.; Lu, R.; Zhu, X.; Yang, W. *J. Mater. Chem. A* 2017, **5**, 19836.
- [16] Chen, Z. L.; Ha, Y.; Liu, Y.; Wang, H.; Yang, H. Y.; Xu, H. B.; Li, Y. J.; Wu, R. B. *ACS Appl. Mater. Interfaces* 2018, **10**, 7134-7144.
- [17] Deng, S.; Zhong, Y.; Zeng, Y.; Wang, Y.; Wang, X.; Lu, X.; Xia, X.; Tu, J. *Adv. Sci.* 2018, **5**, 1700772.
- [18] Zhou, Y.; Wang, Z.; Pan, Z.; Liu, L.; Xi, J.; Luo, X.; Shen, Y. *Adv. Mater.* 2018, 1806769.

- [19] Xiao, K.; Zhou, L.; Shao, M.; Wei, M. *J. Mater. Chem. A* 2018, **6**, 7585-7591.
- [20] Yu, Z. Y.; Lang, C. C.; Gao, M. R.; Chen, Y.; Fu, Q. Q.; Duan, Y.; Yu, S. H. *Energy Environ. Sci.* 2018, **11**, 1890.